CONF-881202--1

The submitted manuscript has been authored by a contractor of the U. S. Government under contract No. W-31-109-ENG-38. Accordingly, the U. S. Government retains a nonexclusive, royalty-free license to publish or reproduce the published form of this contribution, or allow others to do so, for U. S. Government purposes.

CONF-881202--1

DE89 009850

AN EXPERIMENTAL STUDY OF TWO-PHASE NATURAL CIRCULATION IN AN ADIABATIC FLOW LOOP

Michael J. Tan, George A. Lambert, and Mamoru Ishii

Reactor Analysis and Safety Division
Argonne National Laboratory
9700 South Cass Avenue
Argonne, Illinois 60439 U.S.A.

Abstract

An experimental investigation was conducted to study the two-phase flow aspect of the phenomena of interruption and resumption of natural circulation, two-phase flow patterns and pattern transitions in the hot legs of B&W light water reactor systems. The test facility was a scaled adiabatic loop designed in accordance with the scaling criteria developed by Kocamustafaogullari and Ishii [3]. The diameter and the height of the hot leg were 10 cm and 5.5 m, respectively; the working fluid pair was nitrogen-water. The effects of the thermal center in the steam generators, friction loss in the cold leg, and configuration of the inlet to the hot leg on the flow conditions in the hot leg were investigated by varying the water level in a gas separator, controlling the size of opening of a friction loss control valve, and using two inlet geometries. Methods for estimating the the distribution parameter and the average drift velocity are proposed so that they may be used in the application of one-dimensional drift-flux model to the analysis of the interruption and resumption of natural circulation in a similar geometry.

1. INTRODUCTION

The severity of the accident that occurred at Three Mile Island Unit-2 plant has increased interest in the thermal-hydraulic characteristics of the primary system in a pressurized water reactor (PWR) following a small-break loss-of-coolant accident (SBLOCA). In general, the loss of primary system fluid resulting from a small break is reflected in the draining of the pressurizer fluid inventory. The primary system depressurizes gradually during the pressurizer fluid drainage phase and rapidly to the saturation pressure at the hottest region in the primary system once the pressurizer fluid depletes completely. Meanwhile, single-phase natural circulation in the liquid-filled primary loop occurs to provide an effective means of primary heat removal. Owing to the unique configuration of the primary system and the once-through steam generators of a Babcock and Wilcox (B&W) reactor system which entails the use of two elevated hot legs, each consisting mainly of a vertical riser section and a 180 degree U-bend at the top of the riser section (see Figure 1), a particular phenomenon following pressurizer fluid drainage in a SBLOCA in such a system is the likely aggregation of vapor and noncondensible gas around the U-bend of the hot leg so a leveled liquid-vapor interface in the piping downstream of the U-bend may be established. For high rates of loss of

MASTER

DISTRIBUTION OF THIS DOCUMENT IS UNLIMITED

the primary fluid inventory, the level decreases rapidly so circulation may be permanently interrupted. For intermediate rates of loss of the primary fluid inventory, the rate of decrease of the hot-leg phase separation level is slower and the flow interruption may be intermittent. In the light of this, reexamination of the scaling criteria for scale models of prototypical B&W reactor systems concerning the various transient two-phase flow phenomena which may occur during the natural circulation phase of a SBLOCA have been taken up by a number of investigators [1,2]. The set of criteria developed by Ishii and Kataoka [1] was extended and applied by Ishii and Kocamustafaogullari [3] to evaluate the pertinent design parameters of the multiple-loop integral system test (MIST) facility which includes a 2 (hot legs) X 4 (cold legs) simulation loop [4]. In view of certain difficulties in scaling up the data from the 2 X 4 loop used in the MIST to the simulated prototypical reactor system, a supporting experimental program was initiated at Argonne National Laboratory to address the issues of interruption and resumption of natural circulation, flow instability, and two-phase flow patterns and pattern transitions [5,6].

The experimental investigation described herein is the extension of the previous work by Ishii and coworkers [5,6]. The test facility was a scaled down adiabatic loop with one hot leg and one cold leg; the working fluid pair was nitrogen-water. Section 2 contains a detailed description of the test facility. Two series of experiments, which differed only in the configuration of the inlet to the riser section, were performed. In the first series of experiments, the nitrogen gas was injected directly into the vertical riser section of the hot leg whereas in the second of experiments, the vertical riser section was preceded by a horizontal leg so that the two-phase mixture of nitrogen and water flowed through the horizontal leg before entering the vertical riser section. The results of these two series of experiments are discussed in Section 3.

2. APPARATUS AND PROCEDURE

A schematic diagram of the experimental facility, which was designed in accordance with the scaling criteria developed by Kocamustafaogullari & Ishii [3] is shown in Figure 2. A set of operating parameters typical for the experimental loop is compared with that for a prototypical PWR operating at 2% of full power output, 4.7 Mpa, and 260°C in Table I. As shown in Figure 2, the gas delivery system consisted of high pressure gas cylinders, pressure regulators, flow control valves, rotameters, and a gas injector. The gas injector was made of six hundreds twenty-one 0.15 mm I.D. stainless steel hypodermic tubes. The flow loop itself included a bubble chamber corresponding to the reactor core, a riser section and an inverted U-bend section simulating the hot leg of the primary loop, a gas separator simulating the once-through steam generator, a downcomer section and a return section simulating the cold leg of the primary loop.

The bubble chamber, riser and U-bend sections were all composed of 102 mm I.D. Corning Pyrex glass pipes and fittings. The bubble chamber was 356 mm high and was mounted on top of the gas injector. The riser section comprised five subsections. The heights of the four upper ones were, from top to bottom, 305 mm, 1524 mm, 1524 mm, and 1219 mm, respectively. For the first

the second series of experiments the lowermost subsection included a horizontal leg; its vertical height was 432 mm and the distance between the axis of the four upper subsections and that of the bubble chamber was 619 mm. The U-bend section consisted of two 90° sweep elbows. Pressure taps were installed between the subsections of the riser section, between the topmost subsection of the riser section and the U-bend section, and between the bottommost subsection of the riser section and the bubble chamber. The pressure taps were made of 13 mm thick 102 mm I.D. brass rings. The gas separator was made of 203 mm I.D. acrylic plastic pipe and had a total height of 970 mm. The downcomer section consisted of two subsections: the upper one was composed of a piece of 610 mm long 51 mm I.D. Corning Pyrex glass pipe and fittings while the lower one was made of 52 mm I.D. PVC pipes and fittings. The return section was entirely made of PVC pipes and fittings. A gate valve was installed in the return section to study the effect of variation of the friction loss in the cold leg on the flow behavior in the hot leg. A paddle-wheel type flow meter was also installed in the return section for measuring the liquid flow rates. Five strain gauge wet/wet differential pressure transducers were used to measure the pressure difference across each subsection of the riser section.

At the start of each experimental run water from the local water supply system was pumped into the flow loop until it filled the loop and reached the predetermined level in the expansion tank. The opening of the friction loss control valve was set at the desired position. The valves controlling the flow of nitrogen from the gas cylinders into the loop and the valves controlling the flow of nitrogen from the separator to the atmosphere were adjusted concurrently until the nitrogen flow rate and water level in the separator remained steadily at the desired values. The readings from the rotameters, liquid flow meter, pressure gauges, and differential pressure transducers were then recorded.

3. RESULTS AND DISCUSSION

The controllable parameters in the experiments are the gas volumetric flux, the size of opening of the friction loss control valve, and the level of water in the separator. It is noted that owing to the drop in pressure the gas volumetric flux increases along the riser section. For definitiveness the term gas volumetric flux will henceforth pertain to the gas volumetric flux at the inlet to the riser section which was determined from the flow rate data indicated on the rotameter in conjunction with the pressure data from the pressure gauge installed at the exit of the series of rotameters and the pressure data from the pressure gauge installed at the inlet to the riser section. The ranges of the three controllable parameters for ninety-six experimental runs are listed in Table II, where the size of opening of the friction loss control valve is represented in terms of the ratio of the gate valve stem rotations.

3.1 Natural Circulation and Flow Interruption

In general, the circulation of the liquid in the loop is induced by a sufficiently high hydrostatic head difference between the hot-leg riser section and cold-leg return section. The hydrostatic head difference necessary to sustain the circulation is caused by the upward flow of the gas in the riser section. Figures 3 - 8 are plots of the induced liquid volumetric flux

versus the gas volumetric flux for various experimental conditions. As can be seen there, under each experimental condition the induced liquid volumetric flux decreases with decreasing gas volumetric flux so that the state of induced circulation remains stable for gas volumetric fluxes above a certain critical value. As the gas volumetric flux is decreased past the critical value, the hydrostatic head across the riser section becomes insufficient to sustain the circulation so that only the gas is transported over the U-bend section into the separator. Consequently, the level of the gas-liquid two-phase mixture in the hot leg stays at below the U-bend section.

In addition to the permanent flow interruption described above, intermittent interruption of liquid carry-over has also been observed. It occurred when the two-phase mixture was in the slug flow pattern as it entered the U-bend section. Specifically, as a large slug bubble passed through the U-bend, it voided the bend, thereby temporarily interrupting the carry-over of liquid. The time scale of such intermittent flow interruptions was about 1 second. Since the liquid circulation rates measured with the flow meter in the return section were generally steady without significant flow oscillations, it is inferred that the termination of circulation was not a direct consequence of the intermittent flow interruptions.

3.2 Effect of Pressure in the Separator

It is seen from Figures 3 and 4 that the critical gas volumetric flux increases with decreasing liquid level in the separator under otherwise similar experimental conditions. Moreover, at fixed values of gas volumetric flux and opening of friction loss control valve the induced liquid volumetric flux decreases with decreasing liquid level in the separator. Since by virtue of the presence of the expansion tank the pressure at the bottom of the downcomer is maintained virtually constant for all experimental runs, a decrease in the liquid level in the separator results in an increase in the pressure in the separator and a decrease in the hydrostatic head across the riser section. To the extent that the circulation of the liquid is induced by the hydrostatic head difference between the hot-leg riser section and the cold-leg return section, the observed effect of the liquid level in the separator on the critical gas volumetric flux and the induced liquid volumetric flux indicates that the pressure or the liquid level in the once-through steam generator is an important factor in the study of flow instability in the primary loop.

3.3 Effect of Friction Loss in the Cold Leg

The variation of the friction loss in the cold leg was effected by adjusting the size of opening of the gate valve installed in the return section of the test loop. Calibration of the gate valve showed that the friction loss across the valve increases by an order of magnitude as the size of opening of the valve is reduced from fully open to 1/4 open, or from 1/4 open to 1/8 open, or from 1/8 open to 1/16 open, see Refs. [5,6]. Figures 5 - 7 indicate that not until the friction loss across the gate valve is increased by three orders of magnitude does the size of opening of the valve have a significant effect on the value of the critical gas volumetric flux and the induced liquid volumetric flux. This implies that flow behavior in the primary loop is less sensitive to the variation of friction loss in the cold leg than to the variation of the water level in the separator.

3.4 Effect of Geometry of the Inlet Section

The effect of the geometry of the inlet to the hot leg on the induced liquid volumetric flux and the occurrence of permanent flow interruption were studied through the use of two inlet geometries of the riser section in the test loop. One had a straight inlet through which the two-phase mixture of nitrogen gas and water flowed vertically from the bubble chamber into the riser section whereas the other had an elbow inlet preceded by a horizontal leg of approximately 500 mm in length so that the two-phase mixture of nitrogen and water flowed from the bubble chamber through the horizontal leg and elbow before entering the vertical riser section.

It is seen from Figure 8 that the gas flux needed to induce and sustain the circulation of liquid in the test loop under similar experimental conditions is higher when the elbow inlet was used than when the straight inlet was used. This difference is mainly due to the effect of the inlet geometry on the two-phase flow regimes and on the void fraction in the hot leg.

3.5 Flow Patterns and Pattern Transitions

The flow patterns observed in the riser section are bubbly flow and slug flow. Furthermore, two bubbly flow patterns are distinguishable based upon the size and shape of the bubbles; if the majority of bubbles are large so that they are shaped like spherical caps with jagged tails, the relevant flow pattern is qualified as cap-bubbly flow whereas if the majority of bubbles are small and nearly spherical, the revelent flow pattern is simply referred to as bubbly flow. Both types of bubbly flow were observed in the first series of experiments, but by contrast the pattern of bubbly flow in the second series of experiments was always cap-bubbly flow. It was observed that the small bubbles generated in the bubble chamber tended to coalesce in the horizontal leg of the inlet. Thus the flow pattern there became either plug flow where a chain of gas plugs traveled in the upper half of the pipe or completely stratified flow. As the direction of flow of the two-phase mixture was turned from horizontal to vertical at the 90° sweep elbow, spherical cap bubbles or slugs were formed with trailing smaller bubbles.

The axial location where the transition of flow pattern from cap-bubbly flow to slug flow occurred is plotted against the gas volumetric flux for various experimental conditions in Figures 9 and 10. It is seen that the transition locations are fairly independent of the three controllable parameters used in the present study.

3.6 Distribution of Void Fraction

For each experimental run the distribution of void fraction over the length of the riser section was determined from the data from the differential pressure transducers. Specifically, for the first series of experiments the data from the lower four differential pressure transducers were used to approximate the void fractions as third-degree polynomials in length whereas for the second series of experiments the data from the middle three differential pressure transducers were used to approximate the void fractions as second-degree polynomials in length.

The void fraction as a function of length along the riser section for two typical experimental runs are showm in Figures 11 and 12. In general, in the first series of experiments the void fractions decrease at first along the lower part of the riser section, reach a minimum, and then start to increase along the upper part of the riser section whereas in the second series of experiments the void fractions increase monotonically along the entire length of the riser section. As already noted in the previous section, owing to the stratification of the flow in the horizontal leg and the presence of the elbow, the flow of the two-phase mixture in the riser section with the elbow inlet was always in the cap-bubbly flow and slug flow patterns. Consequently, the bubbly flow pattern was able to persist longer in the riser section with the straight inlet. Since the relative velocity between the phases is lower in the bubbly flow pattern than in the slug flow pattern, the void fraction of the two-phase mixture is higher in the bubbly flow pattern than in the slug flow pattern. Thus, the occurrence of the valley-shaped void fraction distributions in the experimental runs performed with the riser section with the straight inlet appears to be attributable to the transition of flow pattern from (cap-)bubbly flow to fully developed slug flow.

It is straightforward to show that in a one-dimensional gas-liquid two-phase flow the void fraction $\langle\alpha\rangle$, the gas volumetric flux $\langle j_g\rangle$ and the liquid volumetric flux $\langle j_f\rangle$ are related by

$$\frac{\langle j_g\rangle}{\langle\alpha\rangle} = C_0\langle j\rangle + \langle\langle V_{gj}\rangle\rangle \ , \tag{1}$$

where $\langle j\rangle$ is the total volumetric flux given by

$$\langle j\rangle = \langle j_g\rangle + \langle j_f\rangle \ , \tag{2}$$

and C_0 and $\langle\langle V_{gj}\rangle\rangle$ are parameters defined respectively by

$$C_0 = \frac{\langle\alpha j\rangle}{\langle\alpha\rangle\langle j\rangle} \ , \tag{3}$$

$$\langle\langle V_{gj}\rangle\rangle = \frac{\langle\alpha(v_g - j)\rangle}{\langle\alpha\rangle} \ . \tag{4}$$

The two parameters C_0 and $\langle\langle V_{gj}\rangle\rangle$ have particular relevance to the one-dimensional drift-flux model for two-phase flows and are commonly referred to as the distribution parameter and the average drift velocity respectively [7]. They are evaluated either directly from the measurements of void fractions at several different gas and liquid volumetric fluxes or from some empirical correlations. For gas-liquid two-phase flows in vertical pipes, the void fractions and the gas volumetric fluxes are generally functions of the axial position. It follows from their definitions, eqs. (3) and (4), that C_0 and $\langle\langle V_{gj}\rangle\rangle$ are also generally functions of the axial position. The values of C_0 and $\langle\langle V_{gj}\rangle\rangle$ at a given axial position can be obtained from the slope and the intercept of the straight line which fits the data points in a plot of $\langle j_g\rangle/\langle\alpha\rangle$ versus $\langle j\rangle$. This procedure of evaluating C_0 and $\langle\langle V_{gj}\rangle\rangle$ is

illustrated by Figures 13 - 16 wherein the datum plane refers to the bottom plane of the vertical riser section. In Table III are listed the values of C_0 and $\langle\langle V_{gj} \rangle\rangle$ thus obtained at eleven axial locations along the riser section. It is seen therein that C_0 and $\langle\langle V_{gj} \rangle\rangle$ are indeed functions of the axial position. In the light of the possible application of the one-dimensional drift-flux model to the analysis of the interruption and resumption of natural circulation, each set of values of of C_0 and $\langle\langle V_{gj} \rangle\rangle$ in Table III was fitted into a third-degree polynomial in axial position z to give the following correlations:

$$C_0 = \begin{cases} 2.043 + 5.608z^* - 14.131z^{*2} + 9.245z^{*3} & \text{for straight inlet} \\ 2.014 - 1.239z^* + 1.307z^{*2} - 0.379z^{*3} & \text{for elbow inlet} \end{cases} \tag{5}$$

$$\langle\langle V_{gj} \rangle\rangle^* = \begin{cases} 0.803 - 3.837z^* + 14.838z^{*2} - 11.827z^{*3} & \text{for straight inlet} \\ 2.402 - 1.557z^* + 1.896z^{*2} - 0.652z^{*3} & \text{for elblow inlet} \end{cases} \tag{6}$$

where $\langle\langle V_{gj} \rangle\rangle^*$ and z^* are scaled (nondimensionalized) quantities given by

$$\langle\langle V_{gj} \rangle\rangle^* = \langle\langle V_{gj} \rangle\rangle \left[\frac{\rho_f^2}{\sigma g(\rho_f - \rho_g)} \right]^{1/4} \tag{7}$$

$$z^* = z/H \, , \tag{8}$$

and H is the length from the datum plane to the top of the U-bend.

In view of the singular nature of the leveled gas-liquid interface, the data of the experimental runs in which the circulation of liquid was not sustained were not used in arriving at Table III and eqs. (5) - (6). They are instead treated separately but in a similar fashion to give the four set of values of C_0 and $\langle\langle V_{gj} \rangle\rangle$ in Table IV and the following correlations:

$$C_0 = \begin{cases} 3.162 + 0.049z^* + 7.994z^{*2} - 10.307z^{*3} & \text{for straight inlet} \\ 1.589 + 2.985z^* - 5.693z^{*2} + 2.131z^{*3} & \text{for elbow inlet} \end{cases} \tag{9}$$

DISCLAIMER

This report was prepared as an account of work sponsored by an agency of the United States Government. Neither the United States Government nor any agency thereof, nor any of their employees, makes any warranty, express or implied, or assumes any legal liability or responsibility for the accuracy, completeness, or usefulness of any information, apparatus, product, or process disclosed, or represents that its use would not infringe privately owned rights. Reference herein to any specific commercial product, process, or service by trade name, trademark, manufacturer, or otherwise does not necessarily constitute or imply its endorsement, recommendation, or favoring by the United States Government or any agency thereof. The views and opinions of authors expressed herein do not necessarily state or reflect those of the United States Government or any agency thereof.

$$\langle\langle V_{gj} \rangle\rangle^{*} = \begin{cases} 0.603 - 0.873z^{*} + 3.462z^{*2} - 2.5172^{*3} & \text{for straight inlet} \\ 2.560 - 3.598z^{*} + 5.050z^{*2} - 1.348z^{*3} & \text{for elbow inlet} \end{cases} \quad (10)$$

It is worth noting that in a recent study Kataoka & Ishii [8] suggested several correlations for evaluating C_0 and $\langle\langle V_{gj} \rangle\rangle$ suitable for flow systems in which gas is injected into a pool of stagnant liquid and that the suggested correlations which are appropriate for the experimental parameters used in the present study are independent of the position in the vertical direction. The values of C_0 and $\langle\langle V_{gj} \rangle\rangle$ calculated from such correlations are 1.193 and 42.3 cm/s respectively. They compare favorably with those calculated from runs performed with the elbow inlet in the present study.

4. SUMMARY

An experimental investigation was conducted to study the hydraulic aspect of the phenomena of interruption and resumption of natural circulation, two-phase flow patterns and pattern transitions in the hot legs of prototypical B&W reactor systems. The test facility was a scaled 1 X 1 (one hot leg, one cold leg) adiabatic loop; the working fluid pair was nitrogen-water. Two series of experiments, which differed only in the configuration of the inlet to the riser section, were performed. In the first series of experiments, the nitrogen gas was injected directly into the vertical riser section of the hot leg while in the second of experiments, the vertical riser section was preceded by a horizontal leg so that the two-phase mixture of nitrogen and water flowed through the horizontal leg before entering the vertical riser section. The results are summarized as follows:

(1) Under each experimental condition the induced liquid volumetric flux decreases with decreasing gas volumetric flux. The state of induced circulation remains stable for gas volumetric fluxes above a certain critical value. As the gas volumetric flux is decreased past the critical value, only the gas is transported over the U-bend.

(2) The critical gas volumetric flux increases with decreasing liquid level in the separator under otherwise similar experimental conditions. Moreover, at fixed values of gas volumetric flux and opening of friction loss control valve the induced liquid volumetric flux decreases with decreasing liquid level in the separator. This suggests that the pressure in the once-through steam generator is an important factor in the study of flow instability in the primary loop.

(3) The size of opening of the friction loss control valve had little effect on the value of the critical gas volumetric flux and the induced liquid volumetric flux. This implies that flow instability in the primary loop is less sensitive to the variation of friction loss in the cold leg.

(4) The flow patterns observed in the riser section distinguish themselves into bubbly flow and slug flow. Both bubbly flow and cap-bubbly flow

were observed in the first series of experiments, but the pattern of bubbly flow in the second series of experiments was always cap-bubbly flow.

(5) In the first series of experiments the void fractions decrease at first along the lower part of the riser section, reach a minimum, and then start to increase along the upper part of the riser section whereas in the second series of experiments the void fractions increase monotonically along the entire length of the riser section. This difference in the distributions of void fraction appears to be attributable to the transition of flow pattern from (cap-)bubbly flow to fully developed slug flow.

(6) The the distribution parameter C_0 and the average drift velocity $\langle\langle V_{gj} \rangle\rangle$ may be estimated from eqs. (5)-(10) in the possible application of the one-dimensional drift-flux model to the analysis of the interruption and resumption of natural circulation.

Acknowledgments

The authors would like to express their sincere appreciation to Drs. Richard Y. Lee and N. Zuber for their comments on the subject and support of the program. Part of the experimental runs were carried out by Mr. Samir Abou El-Seoud, who was on a training assignment with a Fellowship from IAEA funded through the National Academy of Sciences - National Research Council. This work was performed under the auspices of the U.S. Nuclear Regulatory Commission.

REFERENCES

1. Ishii, M. and I. Kataoka, "Scaling Laws for Thermal-hydraulic System under Single-phase and Two-phase Natural Circulation," Nucl. Eng. & Design, Vol. 81, pp. 411-425 (1984).

2. Kocamustafaogullari, G. and M. Ishii, "Reduced Pressure and Fluid to Fluid Scaling Laws for Two-Phase Flow Loop," NUREG/CR-4584, ANL-86-19 (1986).

3. Kocamustafaogullari, G. and M. Ishii, "Scaling Criteria for Two-Phase Flow Loop and Their Application to Conceptual 2 X 4 Simulation Loop Design," Nucl. Tech., Vol. 65, pp. 146-160 (1984).

4. Carter, H. R., "MIST Facility Status," Proc. 13th Water Reactor Safety Research Information Meeting, NUREG/CP-0072, Vol. 4, pp. 83-100 (1985).

5. Kim, S.-B. and M. Ishii, "Flow Visualization Experiment on Hot-leg U-bend Two-phase Natural Circulation Phenomena," NUREG/CR-4621, ANL-86-27 (1986).

6. Hsu, J.-T. and M. Ishii, "Experimental Study on Two-phase Natural Circulation and Flow Termination in a Loop," NUREG/CR-4682, ANL-86-32 (1986).

7. Ishii, M., "One-Dimensional Drift-Flux Model and Constitutive Equations for Relative Motion Between Phases in Various Two-Phase Flow Regimes," ANL-77-47 (1977).

8. Kataoka, I. and M. Ishii, "Drift Flux Model for Large Diameter Pipe and New Correlation for Pool Void Fraction," Int. J. Heat Mass Transfer, Vol. 30, pp. 1927-1939 (1987).

TABLE I. TYPICAL OPERATION PARAMETERS FOR THE EXPERIMENTAL LOOP AND A PROTOTYPICAL PWR AT 2% FULL POWER, 4.7 MPa AND 260°C

Parameter	Prototype	Nitrogen-Water Loop	Ratio
Pipe diameter, m	0.915	0.102	1/9
Pipe cross-sectional area, m^2	0.658	0.00817	1/81
Loop height, m	20.74	5.5	1/3.7
Loop volume, m^3	13.65	0.0448	1/300
Gas volumetric flux, m/s	1.07	0.11	1/10
Quality, %	1.67	0.062	1/27
Void fraction, %	27.3	26.4	1
Gas density, Kg/m^3	23.7	1.14	1/21
Liquid density,	786	998	1.27/1

TABLE II. RANGES OF EXPERIMENTAL PARAMETERS

Parameter	Range
Gas volumetric flux, cm/s	up to 20
Opening size of friction loss control valve	1, 1/4, 1/8, 1/16
Water level in separator, cm	25, 30, 51, 64, 76

TABLE III. VALUES OF C_0 AND $\langle\langle V_{gj} \rangle\rangle$ CALCULATED FROM RUNS WITH NATURAL CIRCULATION

Height from Datum Plane, cm	C_0		$\langle\langle V_{gj} \rangle\rangle$, cm/s	
	Straight Inlet	Elbow Inlet	Straight Inlet	Elbow Inlet
0	2.063	2.019	12.7	39.2
40	2.362	1.916	10.1	37.4
80	2.570	1.842	9.0	35.9
120	2.688	1.785	9.1	34.8
160	2.720	1.741	10.4	33.9
200	2.676	1.707	12.8	33.3
240	2.573	1.680	15.7	33.0
280	2.441	1.662	18.8	32.8
320	2.314	1.652	21.3	32.9
360	2.230	1.654	22.2	33.1
400	2.219	1.671	20.9	33.3

TABLE IV. VALUES OF C_0 AND $\langle\langle V_{gj} \rangle\rangle$ CALCULATED FROM RUNS WITH FLOW INTERRUPTION

Height from Datum Plane, cm	C_0		$\langle\langle V_{gj} \rangle\rangle$, cm/s	
	Straight Inlet	Elbow Inlet	Straight Inlet	Elbow Inlet
0	3.174	1.574	9.7	42.1
40	3.190	1.813	9.2	37.4
80	3.302	1.945	9.0	34.2
120	3.452	2.007	9.1	32.1
160	3.611	2.020	9.4	30.9
200	3.755	1.995	10.1	30.3
240	3.860	1.936	10.9	30.3
280	3.901	1.847	11.9	30.9
320	3.852	1.729	12.8	32.2
360	3.697	1.581	13.4	34.1
400	3.440	1.398	13.5	36.8

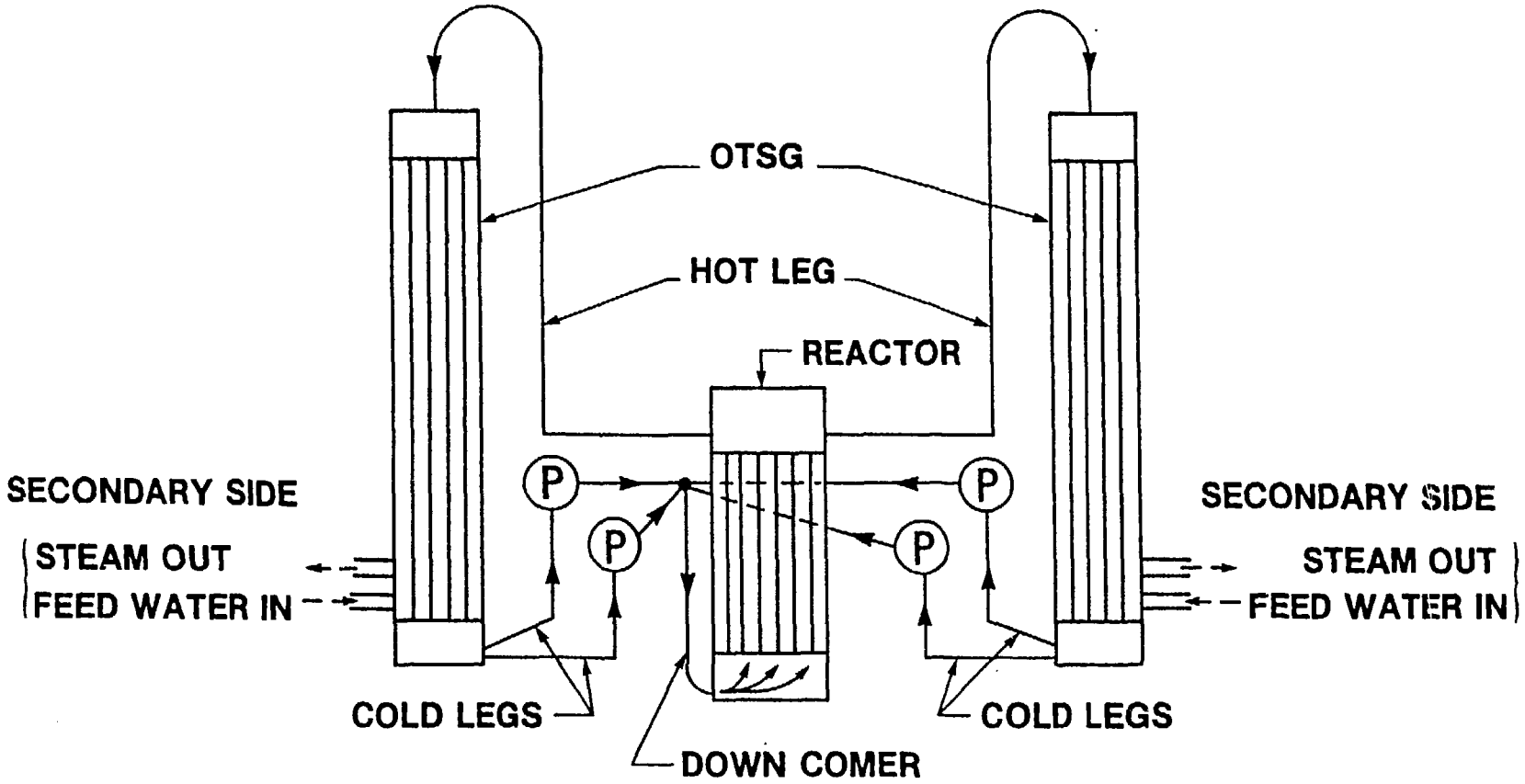

Fig. 1. - Schematic of Babcock and Wilcox Nuclear Reactor System.

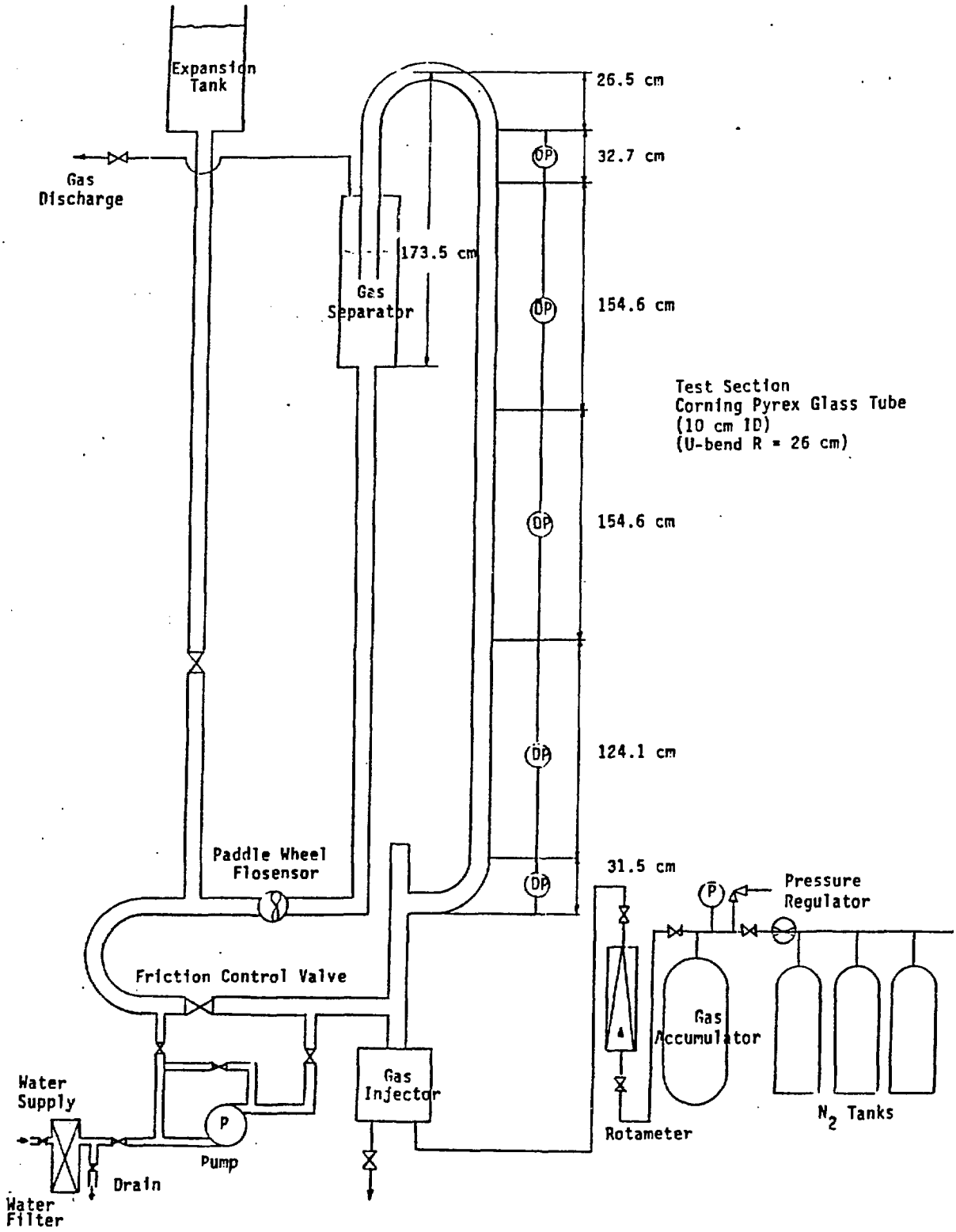

Fig. 2. - Schematic of the Experimental Setup.

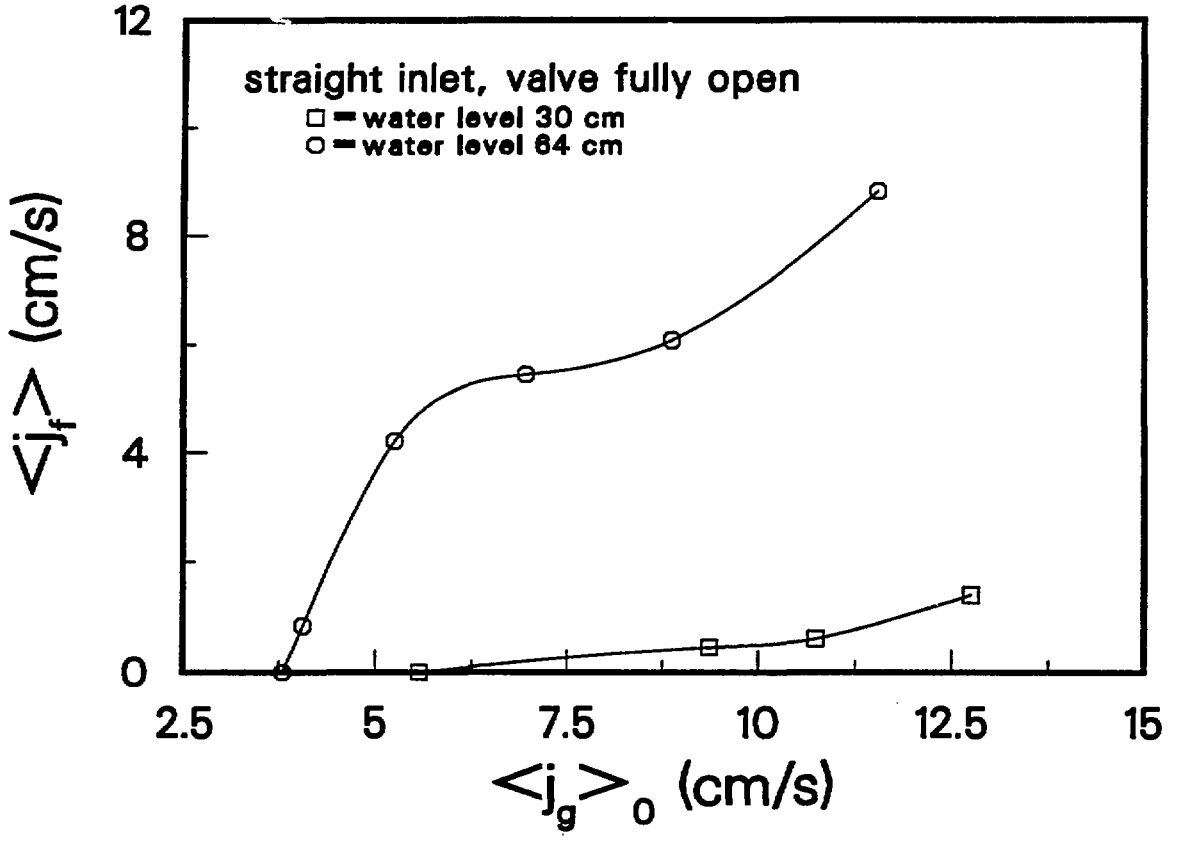

Fig. 3. - Induced Liquid Volumetric Flux vs. Gas Volumetric Flux. Straight Inlet, Friction-Loss Control Valve Fully Open.

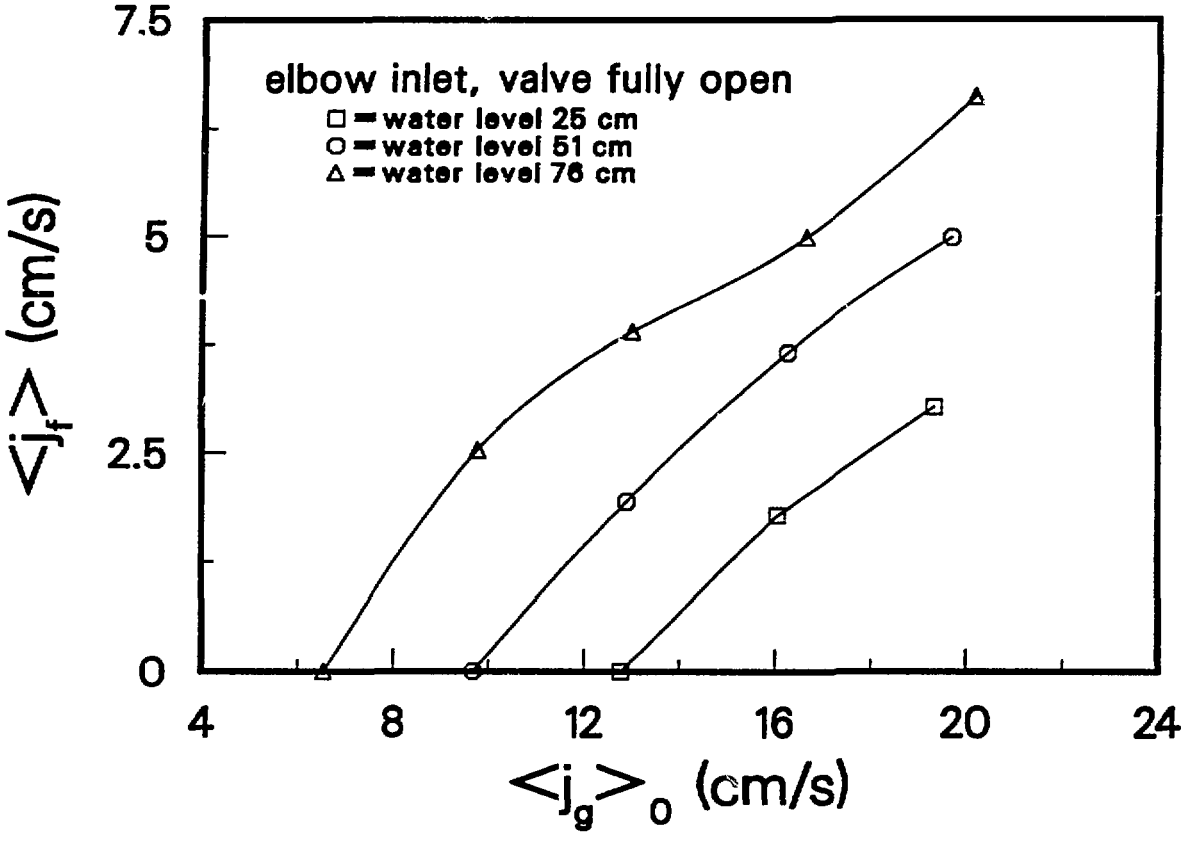

Fig. 4. - Induced Liquid Volumetric Flux vs. Gas Volumetric Flux. Elbow Inlet, Friction-Loss Control Valve Fully Open.

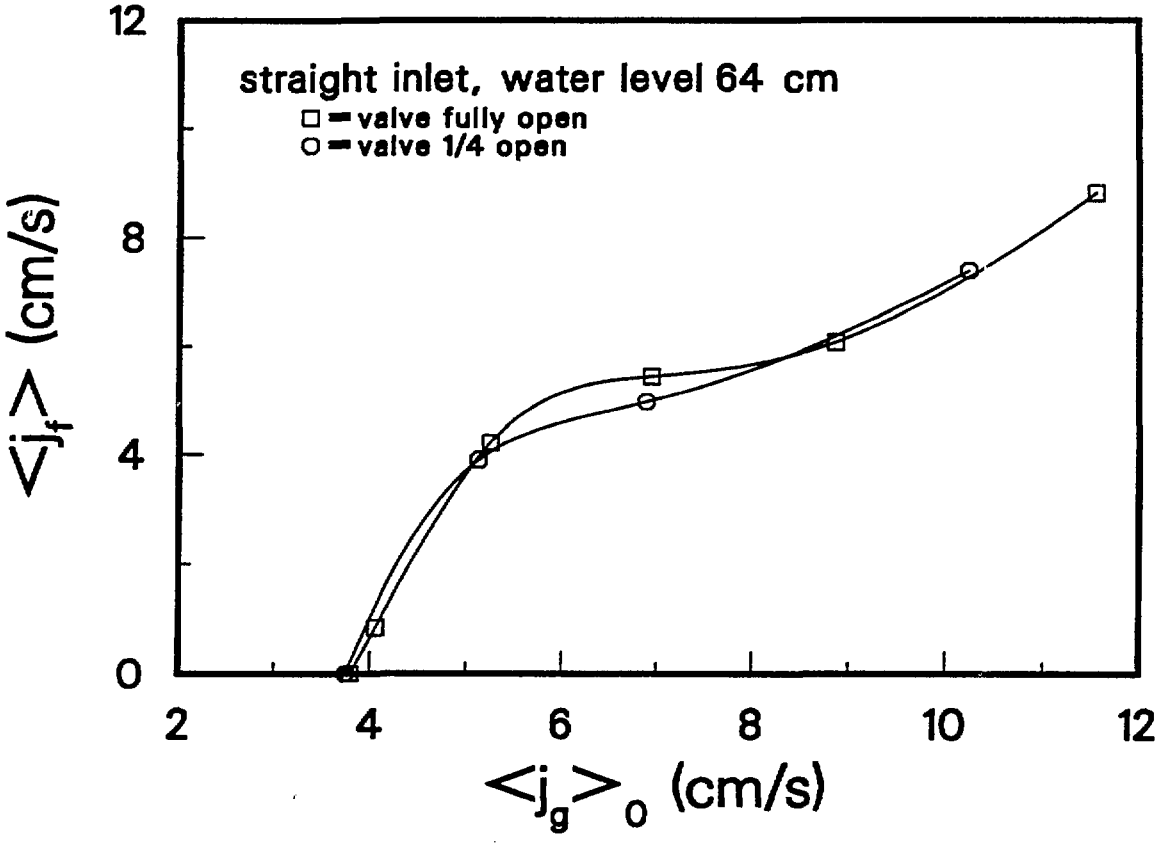

Fig. 5. - Induced Liquid Volumetric Flux vs. Gas Volumetric Flux. Straight Inlet, Separator Water Level 64 cm.

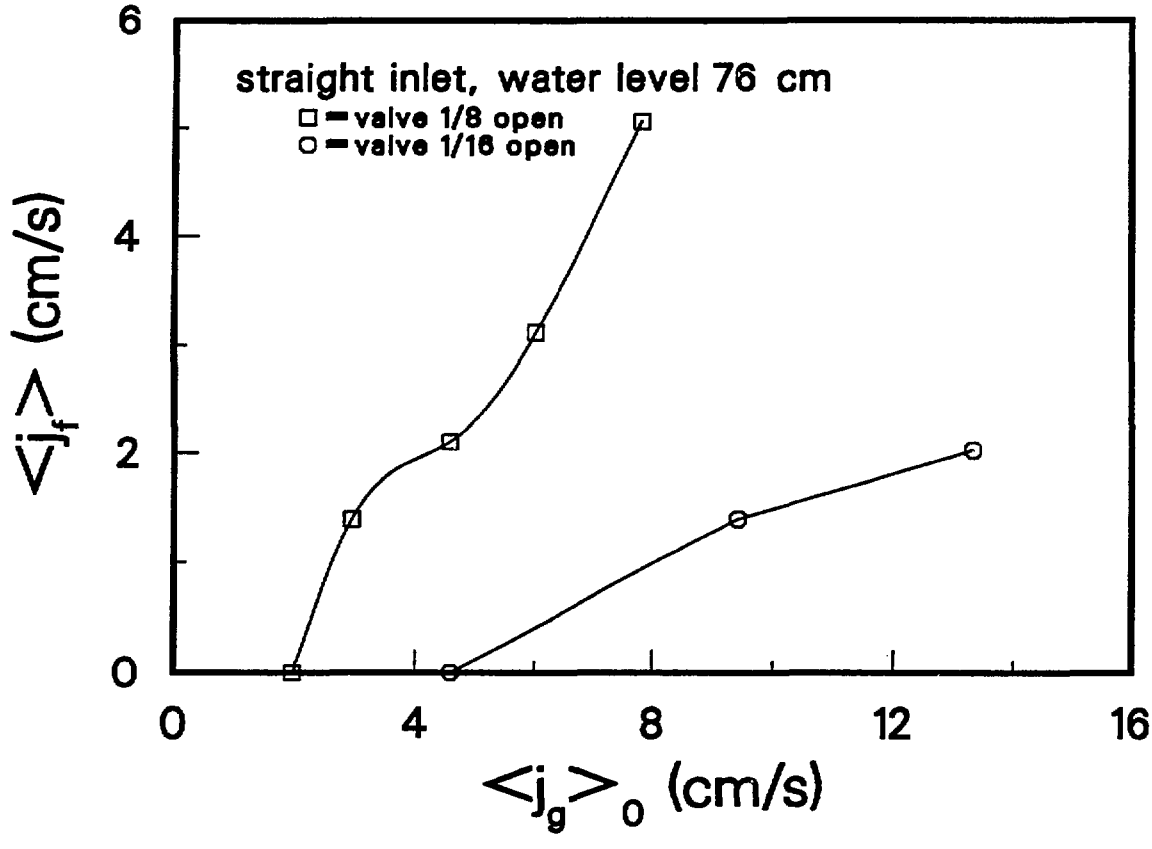

Fig. 6. - Induced Liquid Volumetric Flux vs. Gas Volumetric Flux. Straight Inlet, Separator Water Level 76 cm.

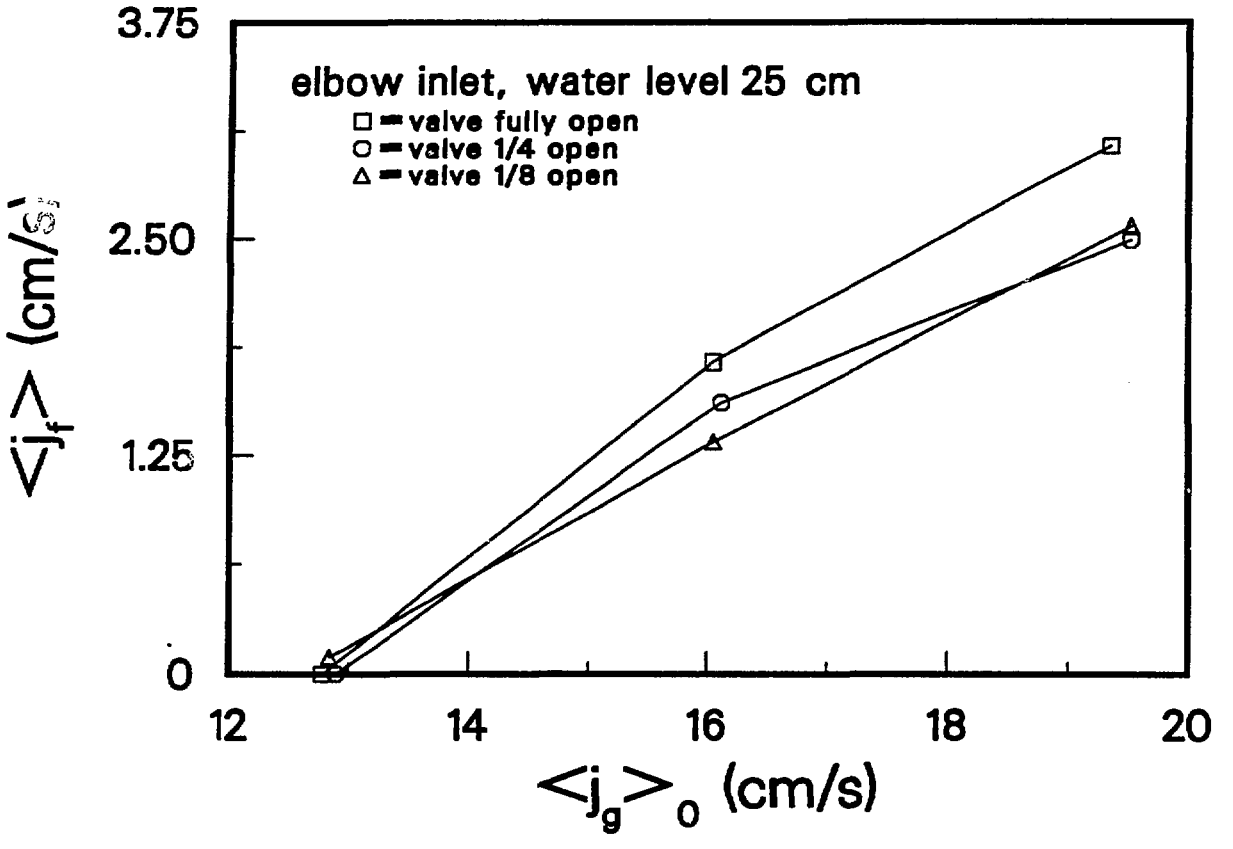

Fig. 7. - Induced Liquid Volumetric Flux vs. Gas Volumetric Flux. Elbow Inlet, Separator Water Level 25 cm.

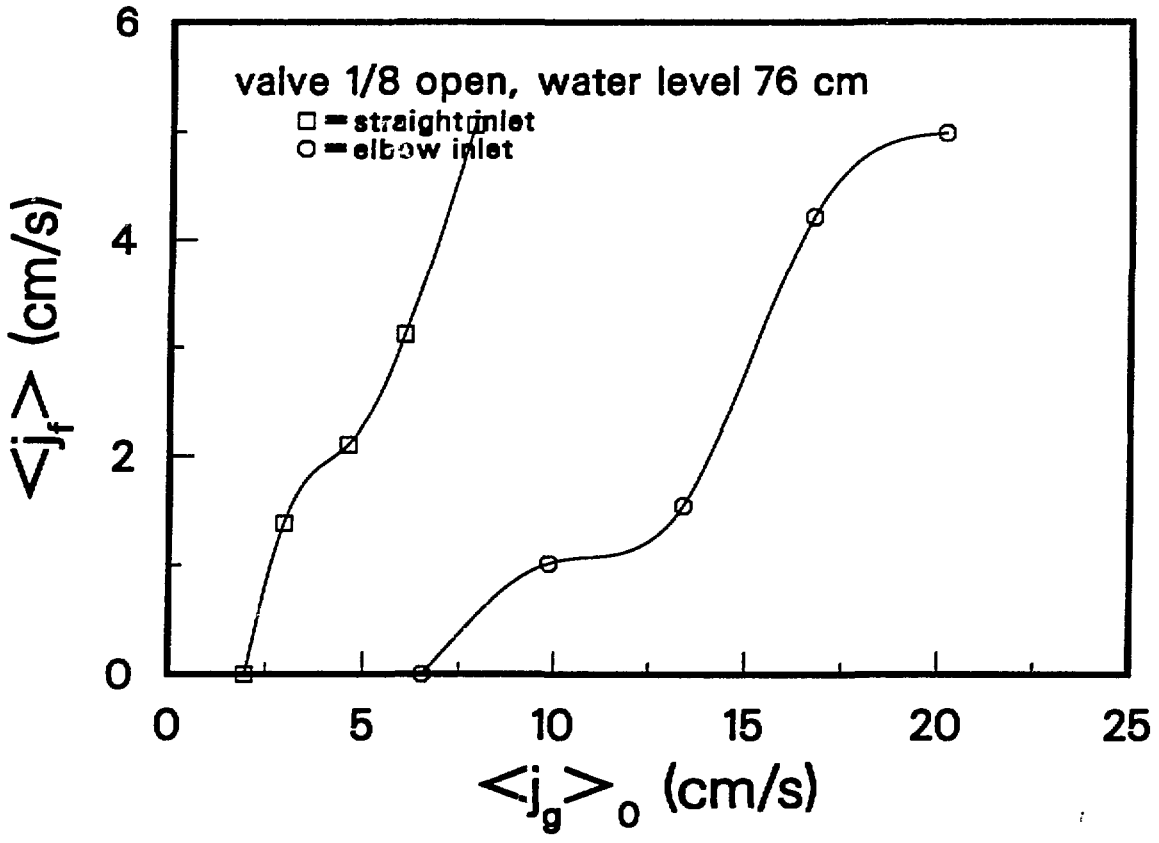

Fig. 8. - Induced Liquid Volumetric Flux vs. Gas Volumetric Flux. Friction-Loss Control Valve 1/8 Open, Separator Water Level 76 cm.

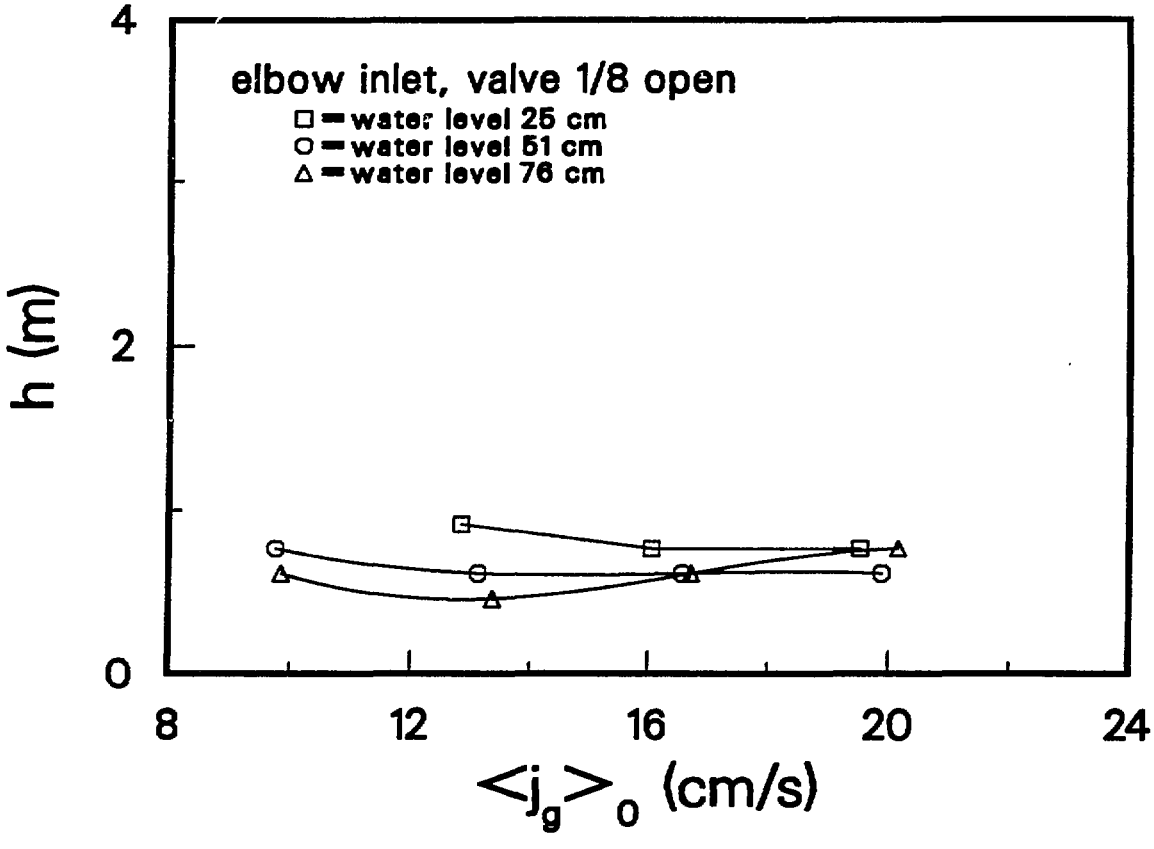

Fig. 9. - Location of Flow-Pattern Transition from Cap-Bubbly Flow to Slug Flow vs. Gas Volumetric Flux. Elbow Inlet, Friction-Loss Control Valve 1/8 Open.

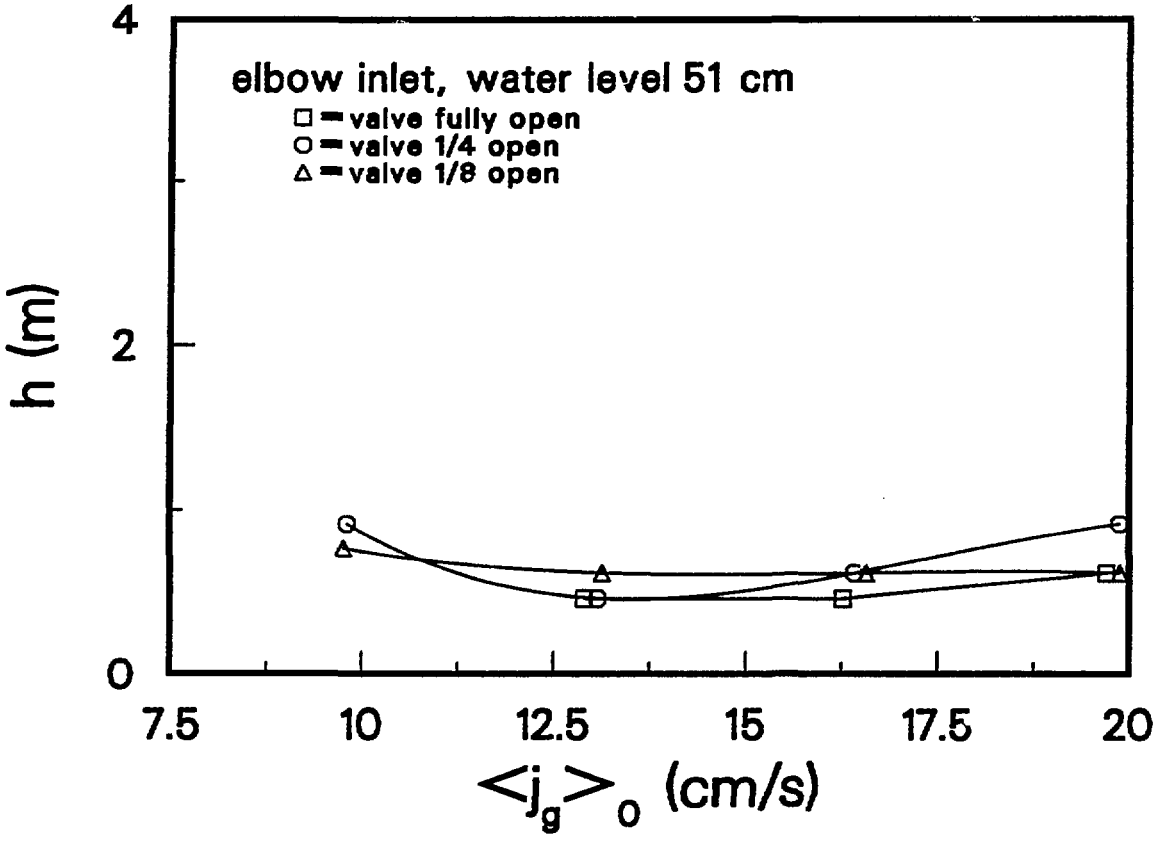

Fig. 10. - Location of Flow-Pattern Transition from Cap-Bubbly Flow to Slug Flow vs. Gas Volumetric Flux. Elbow Inlet, Separator Water Level 51 cm.

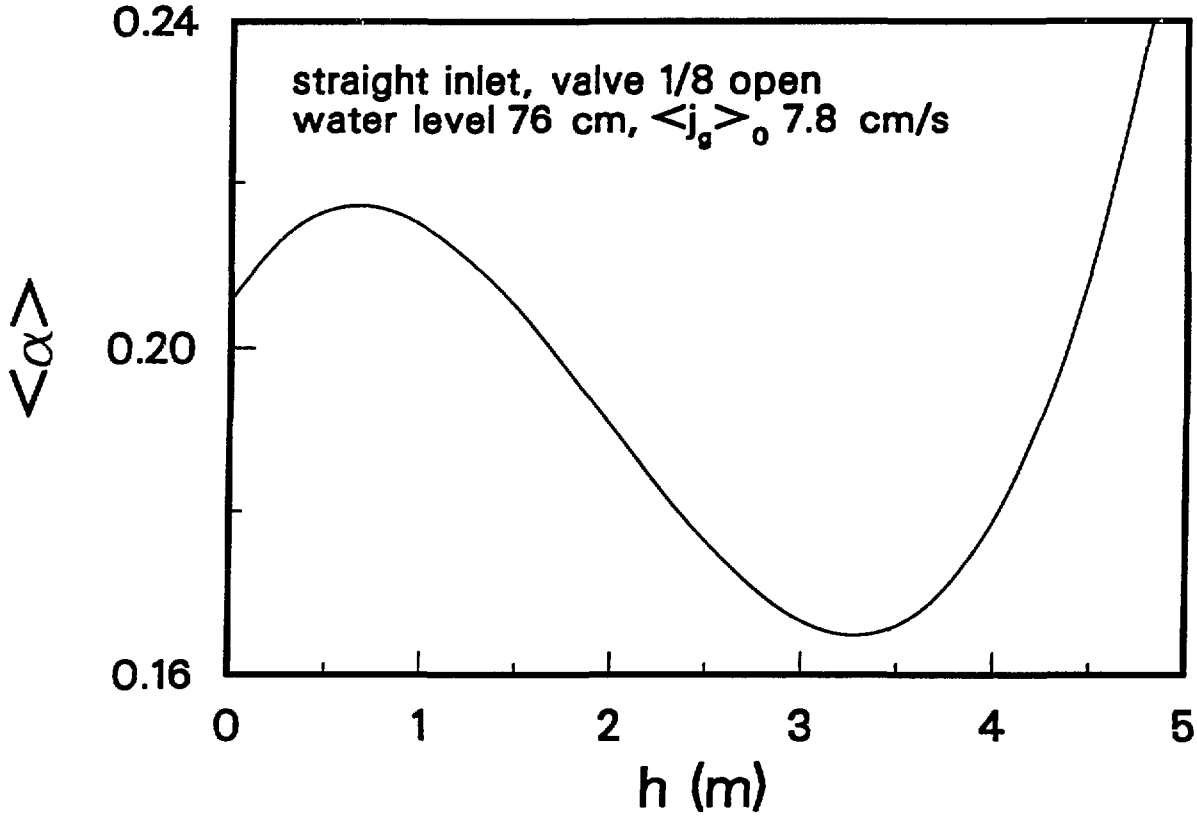

Fig. 11. - Void Fraction as a Function of Length Along the Riser Section. Straight Inlet, Friction-Loss Control Valve 1/8 Open, Separator Water Level 76 cm.

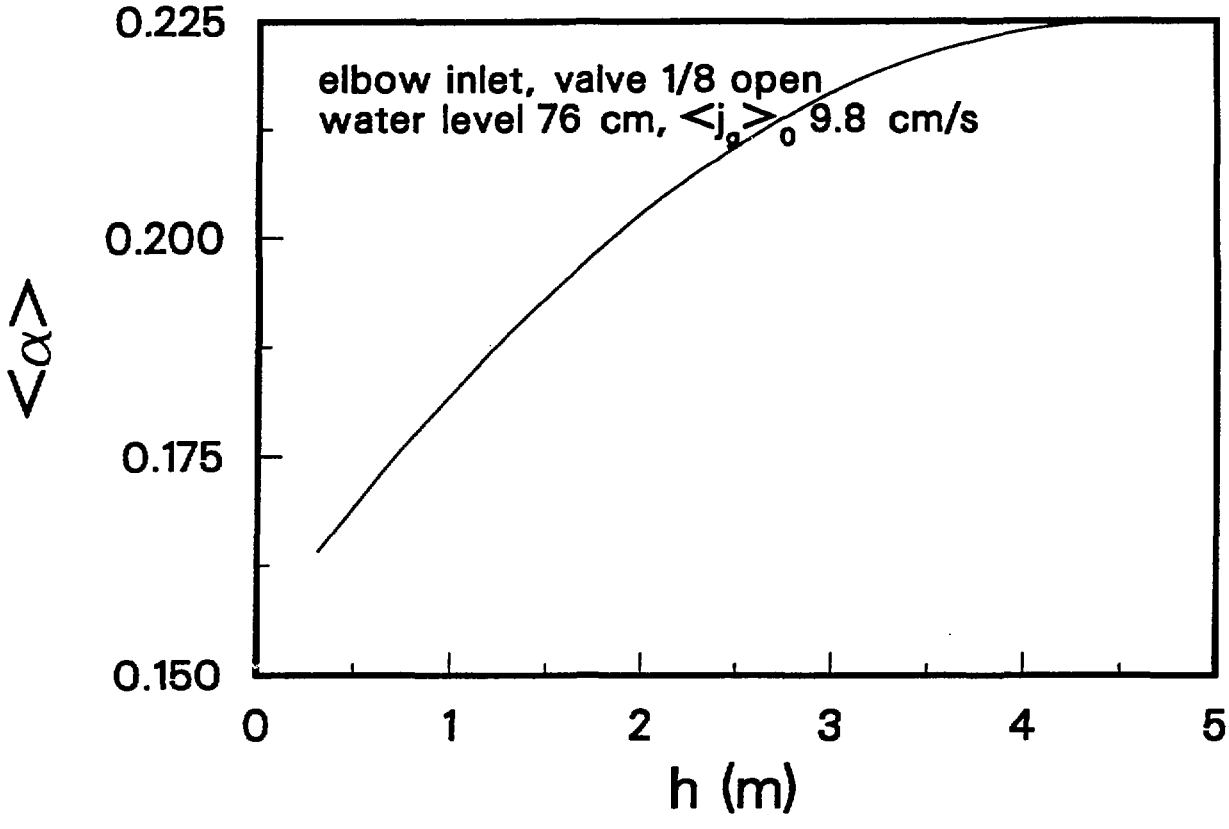

Fig. 12. - Void Fraction as a Function of Length Along the Riser Section. Elbow Inlet, Friction-Loss Control Valve 1/8 Open, Separator Water Level 76 cm.

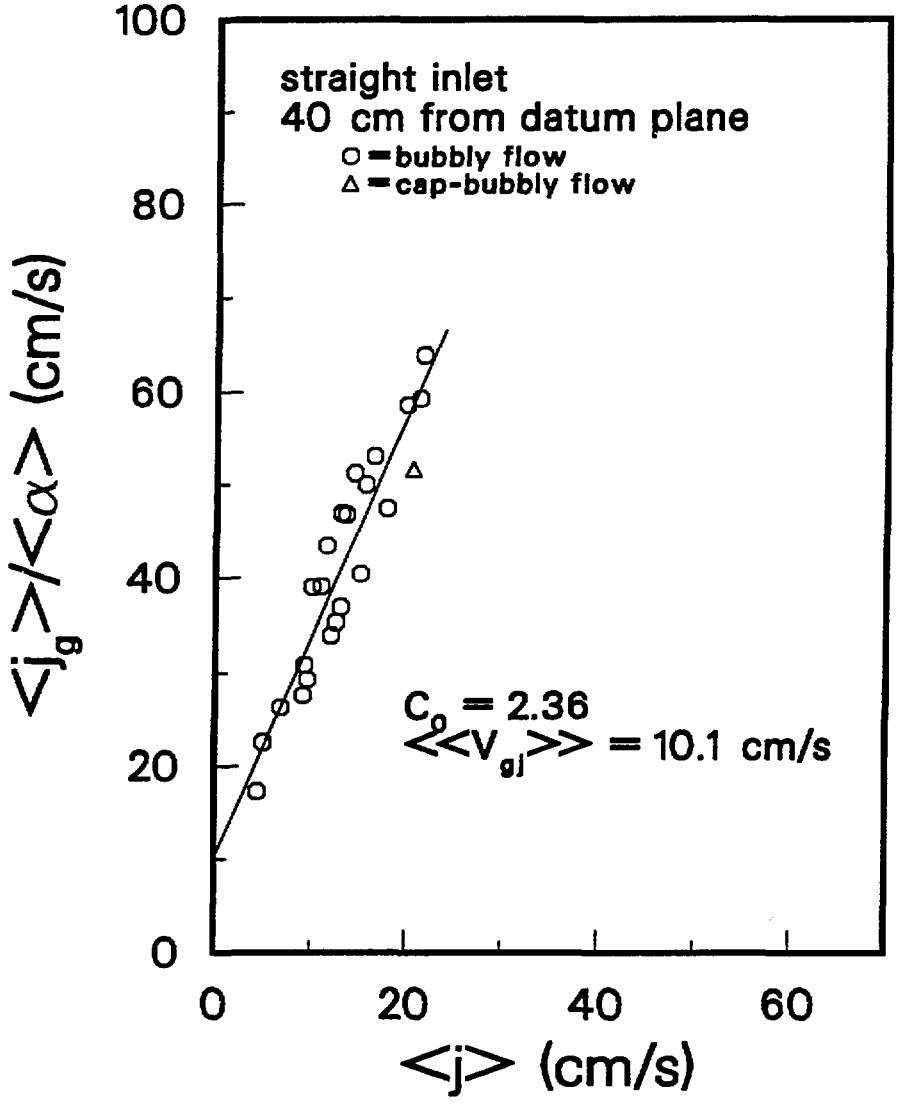

Fig. 13. - $\langle j_g\rangle/\langle\alpha\rangle$ vs. $\langle j\rangle$. Straight Inlet, 40 cm from Datum Plane.

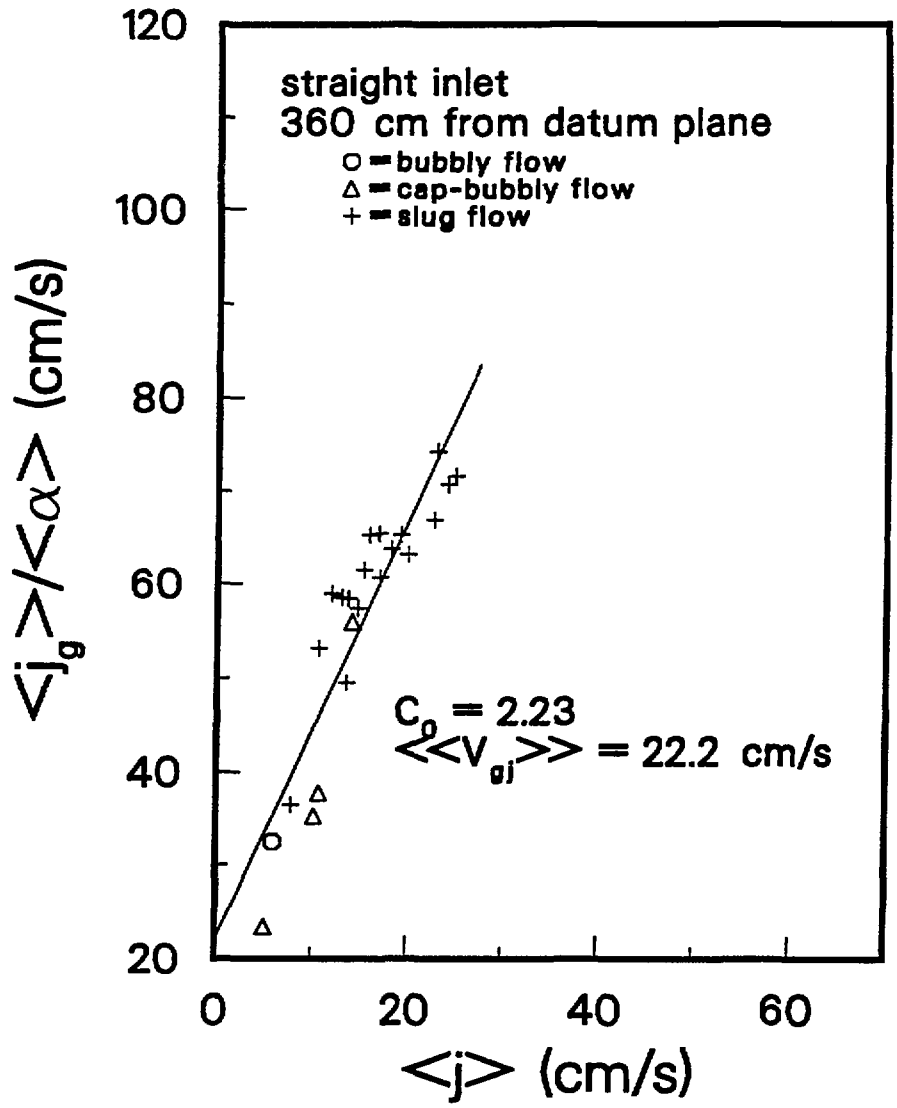

Fig. 14. - $\langle j_g\rangle/\langle\alpha\rangle$ vs. $\langle j\rangle$. Straight Inlet, 360 cm from Datum Plane.

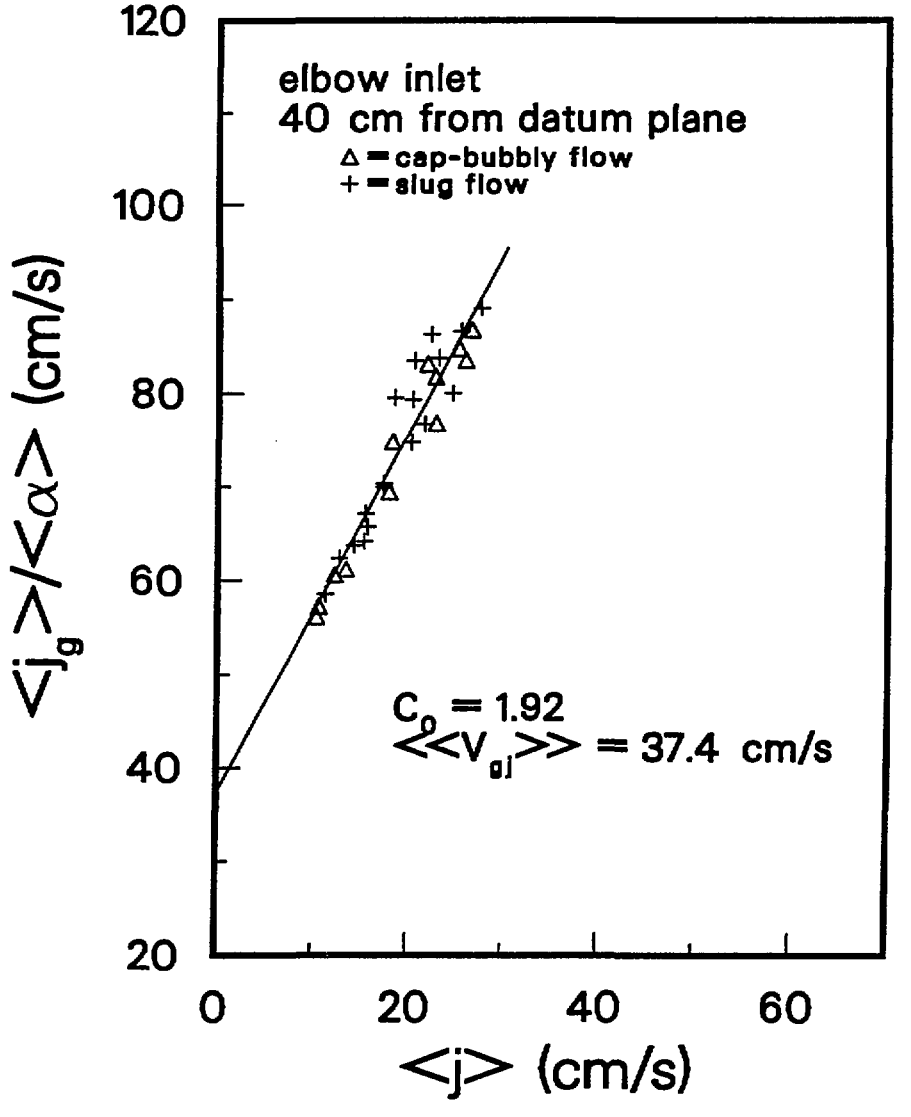

Fig. 15. - $\langle j_g\rangle/\langle\alpha\rangle$ vs. $\langle j\rangle$. Elbow Inlet, 40 cm from Datum Plane.

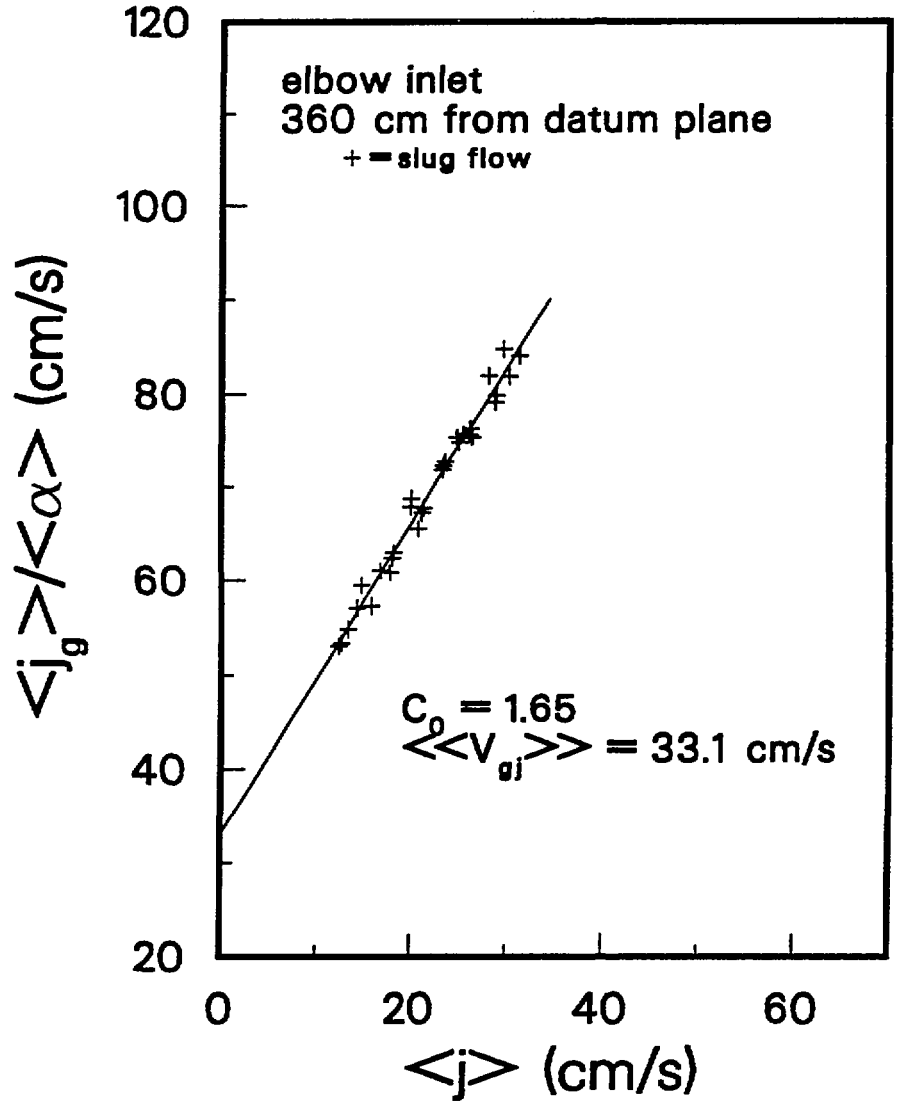

Fig. 17. - $\langle j_g \rangle / \langle \alpha \rangle$ vs. $\langle j \rangle$. Elbow Inlet, 360 cm from Datum Plane.